

# High temperature electrical resistance of substrate-supported single walled carbon nanotubes

C. Thomas Avedisian,<sup>1,a)</sup> Richard E. Cavicchi,<sup>2</sup> Paul M. McEuen,<sup>3</sup> Xinjian Zhou,<sup>3</sup> Wilbur S. Hurst,<sup>2</sup> and Joseph T. Hodges<sup>2</sup>

<sup>1</sup>Sibley School of Mechanical and Aerospace Engineering, Cornell University, Ithaca, New York 14853, USA

<sup>2</sup>Process Measurements Division, National Institute of Standards and Technology, Gaithersburg, Maryland 20899, USA

<sup>3</sup>Department of Physics, Cornell University, Ithaca, New York 14850, USA

(Received 13 August 2008; accepted 1 December 2008; published online 24 December 2008)

We report the electrical characteristics of substrate-supported metallic single walled carbon nanotubes at temperatures up to 573 K over a range of bias voltages ( $V_b$ ) for zero gate voltage in air under atmospheric pressure. Our results show a monotonic increase in resistance with temperature, with an  $I$ - $V_b$  characteristic that is linear at high temperature but nonlinear at low temperature. A theory for electrical resistance is applied to the data which shows that the transition to Ohmic behavior at high temperature is the result of optical phonon absorption rather than acoustic phonon scattering. © 2008 American Institute of Physics. [DOI: 10.1063/1.3052867]

The electrical characteristics of single walled carbon nanotubes (SWNTs) are of interest for a variety of applications (e.g., transistors and interconnects,<sup>1–5</sup> thermal management of electronic systems,<sup>6</sup> biological sensors,<sup>7</sup> thermal therapeutics for cancer treatment,<sup>8</sup> and thermal property measurements<sup>9,10</sup>) and the effect of temperature is important in many of them. A number of studies have reported the electrical resistance of individual SWNTs at low temperatures [ $<300$  K (Refs. 11–17)] and above 300 K for SWNT ropes, sheets, and fibers.<sup>1,11,18,19</sup> Individual *suspended* SWNTs have been taken up to 400 K (Refs. 5, 13, and 14) with the highest temperature—for a multiwalled carbon nanotube—being 523 K.<sup>19</sup>

In this letter we report electrical characteristics of individual *substrate-supported* metallic SWNTs over a range of bias voltage ( $V_b$ ) up to 573 K in air at atmospheric pressure and for zero gate voltage. Substrate support provides greater structural integrity than suspended SWNTs and negative differential conductance (NDC) is not generally exhibited because of reduced self-heating effects.<sup>5,16,20–23</sup> SWNTs are obtained by direct growth across  $\text{FeO}_3/\text{MoO}_2$  catalyst pads placed on a 500 nm  $\text{SiO}_2$  layer with a Si substrate in a chemical vapor deposition process as described previously.<sup>2,15,22,24,25</sup> A 50 nm sublayer of Cr lines 10  $\mu\text{m}$  apart is patterned on top of  $\text{SiO}_2$  and a 50 nm Au layer is patterned on top of Cr. Atomic force microscopy scans showed  $L \approx 11 \pm 1$   $\mu\text{m}$  and tube diameters between 1 and 2 nm.

Devices were electrically probed using an Alessi Rel 4100-A probe station<sup>26</sup> fitted with a Temptronic Thermochuck for heating the tubes. A Keithley 2410 source meter was used to obtain two-terminal current-voltage characteristics under LABView control. The electrical characteristics of metallic SWNTs are reported: one tube (SWNT1) is probed up to  $V_b=2$  V to potentially promote nonlinear effects; the other tube (SWNT2) is limited to  $V_b < 0.05$  V but smaller temperature increments up to 572 K.

Figures 1 and 2 show the variation in current with  $V_b$  for SWNT1 and SWNT2, respectively, at the indicated temperatures (lines are discussed later). At low bias the variation is linear and the resistance ( $R=V_b/I$ ) is independent of  $V_b$  (see inset). As  $V_b$  increases at low temperature for SWNT1, a progressively nonlinear variation with current is found though the saturation current for NDC is predicted<sup>16</sup> to be much higher than the data shown in Fig. 1.

Figures 3 and 4 show the low bias resistance (obtained by linearizing the data in Figs. 1 and 2 for  $V_b < 0.05$  V) for SWNT1 and SWNT2 as a function of temperature. To understand the temperature effects we apply the Landauer–Buttiker formulation,<sup>14,23</sup>  $R=R_c+h/(4q^2)(1+L/\lambda_{\text{eff}})$ , with the current determined from  $i=V_b/R(V_b)$ .  $R_c$ ,  $\lambda_{\text{eff}}$ ,  $h$ ,  $q$ , and  $E_{\text{op}}$  are the electrical contact resistance, total effective mean free path (MFP), Planck’s constant, electric charge, and optical phonon threshold energy, respectively.  $\lambda_{\text{eff}}=1/(1/\lambda_{\text{ac}}+1/\lambda_{\text{op,abs}}+1/\lambda_{\text{op,ems}})$ ,  $\lambda_{\text{ac}}=\lambda_{\text{aco}}T/T_{\text{ac}}$ ,  $\lambda_{\text{op,abs}}=\lambda_{\text{opo}}[n_o(T_o)$

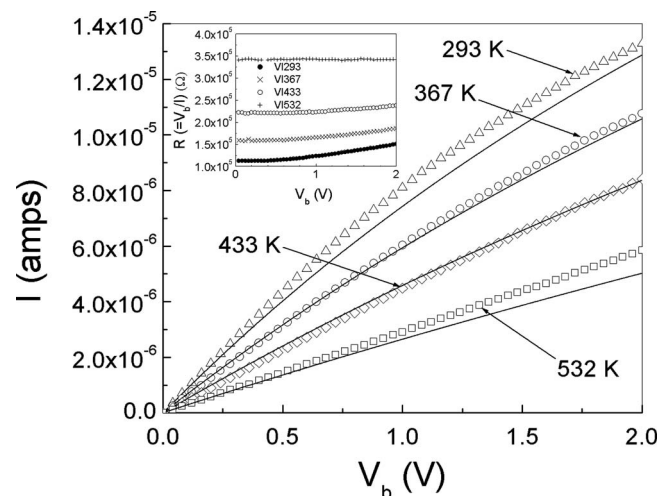


FIG. 1. Variation in current with  $V_b$  for SWNT1 at four temperatures. Predictions (solid lines) correspond to best-fit values of parameters:  $\lambda_{\text{aco}}=650$  nm,  $\lambda_{\text{opo}}=1$  nm,  $E_{\text{op}}=0.31$  eV, and  $R_c=0.0$   $\Omega$ .

<sup>a)</sup>Electronic mail: cta2@cornell.edu.

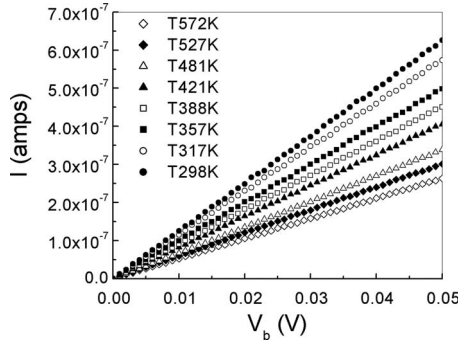


FIG. 2. Variation in current with  $V_b$  for SWNT2 at selected temperatures.

$+1]/n_o(T_{op})$ , and  $\lambda_{op,ems} = 1/(1/\lambda_{ems,abs} + 1/\lambda_{ems,fld})$ , where  $\lambda_{ems,abs} = \lambda_{op,abs} + \lambda_{opo}[n_o(T_o) + 1]/[n_o(T_{op}) + 1]$  and  $\lambda_{ems,fld} = \lambda_d + \lambda_{opo}[n_o(T_o) + 1]/[n_o(T_{op}) + 1]$ .  $\lambda_d = LE_{op}/(q|V_b|)$  is the distance required for electrons to reach  $h_e$ .  $\lambda_{aco}$ ,  $\lambda_{opo}$ , and  $n_o$  are the room temperature acoustic scattering MFP, room temperature optical emission MFP, and number of optical phonons, respectively, where  $n_o = 1/[\exp(E_{op}q/k_B T_{op}) - 1]$ .  $T_{ac}$  and  $T_{op}$  are temperatures associated with acoustic and optical phonons, and  $T_o = 300$  K.

Parameters are determined that best represented the measurements using the STEPIT algorithm.<sup>27–29</sup> A lumped thermal model for the SWNT temperature is used to model the heat flow in the comparatively large aspect ratio SWNTs investigated. Joule heating, assumed to be dissipated to acoustic phonons, is balanced by thermal losses from the SWNT to the surroundings as  $i^2(R - R_c) = Lg(T_{ac} - T_\infty)$ .  $g$  measures the heat loss per unit length to the surroundings and the temperature ( $T_{ac}$ ) corresponds to acoustic phonons.  $T_{ac}$  is related to  $T_{op}$  as<sup>5,9</sup>  $T_{op} = T_{ac} + \alpha(T_{ac} - T_\infty)$ , where  $\alpha$  is the fraction of the total thermal resistance along the SWNT that is associated with optical phonons.<sup>14</sup> The parameters to be determined are  $R_c$ ,  $\lambda_{aco}$ ,  $\lambda_{opo}$ ,  $E_{op}$ ,  $\alpha$ , and  $g$ .

We found that global fits by the algorithm to the SWNT1 and SWNT2  $I-V_b$  data always drove  $g$  to a “large” value and  $\alpha$  to a “small” value which indicates thermal equilibrium,

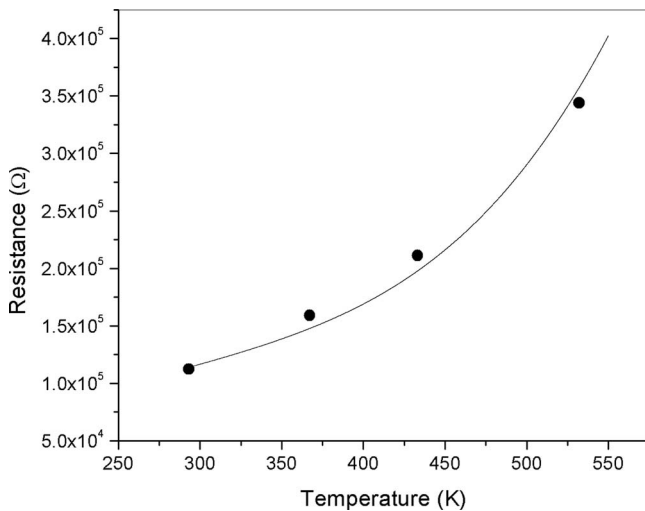


FIG. 3. Variation in electrical resistance with temperature for SWNT1. Measured value (closed circles) is obtained by linearizing the measurements (see Fig. 1) for  $0 < V_b < 0.2$  V. Predicted resistances correspond to  $V_b = 0.01$  V and the following parameters:  $R_c = 0.0$  Ω,  $\lambda_{aco} = 650$  nm,  $\lambda_{opo} = 1$  nm, and  $E_{op} = 0.31$  eV.

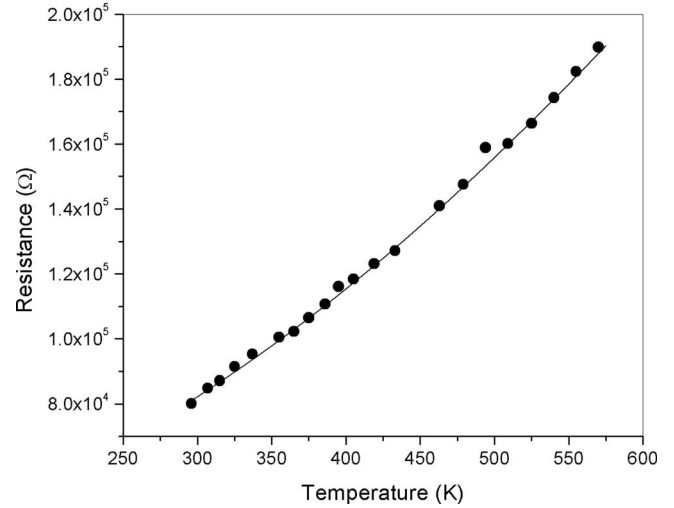


FIG. 4. Variation in electrical resistance with temperature for SWNT2. Measured values (closed circles) are obtained by linearizing the measurements (Fig. 2) for  $0.01 < V_b < 0.05$  V. Predicted resistances correspond to  $V_b = 0.01$  V and the following parameters:  $\lambda_{aco} = 980$  nm,  $\lambda_{opo} = 166$  nm,  $E_{op} = 0.148$  eV, and  $R_c = 0.0$  Ω.

$T_{op} = T_{ac} = T_\infty$ . The extracted  $R_c$  was always very small ( $\ll R$ ). From our fabrication process we may expect that  $R_c \sim 30$  kΩ or less.<sup>15</sup> The extracted room temperature parameters showed little sensitivity to  $R_c$  less than this value.

For SWNT1 we find that  $E_{op} = 0.31$  eV,  $\lambda_{aco} = 650$  nm, and  $\lambda_{opo} = 1$  nm, where  $\lambda_{opo}$  is somewhat small compared to previous estimates<sup>16,22</sup> which could be due to additional scattering mechanisms not considered in the model. Nonetheless, the lines in Fig. 1 show good agreement using these parameters under most conditions (e.g., at low  $V_b$ ). Figure 3 shows the predicted low bias resistance (line; predicted resistances were obtained by linearizing the  $I-V_b$  predictions over  $V_b < 0.05$  V). For SWNT2,  $E_{op} = 0.148$  eV,  $\lambda_{aco} = 980$  nm, and  $\lambda_{opo} = 166$  nm. Using these parameters, Fig. 4 compares the predicted and measured low bias resistances.

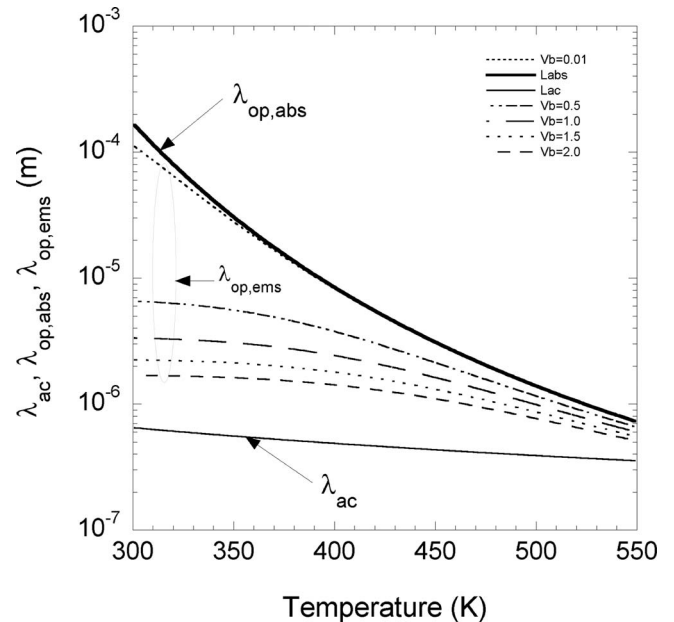


FIG. 5. Variation in MFPs with temperature at various  $V_b$  computed using SWNT1 parameters.

The differing resistance values shown in Figs. 3 and 4 may be traced to  $\lambda_{\text{opo}}$  which could be due to variations in the SWNT chirality which is difficult to control in the manufacturing process, humidity which can influence the relationship between  $V_b$  and current,<sup>30</sup> or variations in tube diameter [i.e., as  $E_{\text{op}} \sim 1/d^2$  (Ref. 31)]. This difference deserves further study. The fact that the two SWNTs have different electrical properties indicates the need for a separate calibration when using a SWNT as a thermometer.

To further understand the role of temperature and bias on electrical characteristics, Fig. 5 shows the computed MFPs using SWNT1 parameters for illustration. At low temperatures ( $\sim 300$  K) and low  $V_b$ , acoustic phonons most influence the flow of current because  $\lambda_{\text{ac}} \ll \lambda_{\text{op,ems}}$  and  $\lambda_{\text{ac}} \ll \lambda_{\text{op,abs}}$  and Ohmic behavior results (since only  $\lambda_{\text{op,ems}}$  depends on  $V_b$ ). As  $V_b$  increases at low temperature,  $\lambda_{\text{op,ems}} \sim \lambda_{\text{ac}}$  and optical emission phonons begin to exert an influence on current and non-Ohmic behavior is found. With increasing temperature,  $\lambda_{\text{op,ems}} \sim \lambda_{\text{op,abs}}$ . It is the  $\lambda_{\text{op,abs}}$  contribution that produces the strong temperature dependence of  $\lambda_{\text{op,ems}}$  seen in Fig. 5 and  $\lambda_{\text{op,abs}}$  rather than  $\lambda_{\text{ac}}$  is responsible for the approach to Ohmic behavior observed in the high temperature data in Fig. 1.

In summary, we found that at “low”  $V_b$  and “high” temperature both SWNTs show Ohmic behavior. Good fits to the data are found, though with substantially different room temperature optical and acoustic MFPs. There appeared to be excellent thermal coupling to the substrate. The results show that changes in optical phonon absorption with temperature, rather than scattering by acoustic phonons, produce the Ohmic behavior at elevated temperatures.

This work was supported in part by the New York State Office of Science, Technology and Academic Research (Dr. Kelvin Lee, Director). The laboratory assistance of Mr. Johannes Kutten is appreciated. The authors also thank Dr. Casey Mungle, Dr. Michael J. Tarlov, and Dr. John Suehle of NIST.

<sup>1</sup>N. R. Franklin, Q. Wang, T. W. Tomblor, A. Javey, M. Shim, and H. Dai, *Appl. Phys. Lett.* **81**, 913 (2002).

<sup>2</sup>P. L. McEuen, M. S. Fuhrer, and H. Park, *IEEE Trans. Nanotechnol.* **1**, 78 (2002).

<sup>3</sup>A. Javey, J. Guo, Q. Wang, M. Linstrom, and J. Dai, *Nature (London)* **424**, 654 (2003).

<sup>4</sup>W. Hoenlein, F. Kreupl, G. S. Duesberg, A. P. Graham, M. Liebau, R. Seidel, and E. Unger, in *Silicon*, edited by P. Siffert and K. Kimmel (Springer, New York, 2004), pp. 477–488.

<sup>5</sup>E. Pop, D. Mann, J. Cao, Q. Wang, K. Goodson, and H. Dai, *Phys. Rev.*

*Lett.* **95**, 155505 (2005).

<sup>6</sup>X. Hu, A. A. Padilla, J. Xu, T. S. Fisher, and K. E. Goodson, *ASME J. Heat Transfer* **128**, 1109 (2006).

<sup>7</sup>K. Besteman, J. O. Lee, F. G. M. Wiertz, H. A. Heering, and C. Dekker, *Nano Lett.* **3**, 727 (2003).

<sup>8</sup>P. Chakravarty, R. Marches, N. S. Zimmerman, A. D. E. Swafford, P. Bajaj, I. H. Musselman, P. Panton, R. K. Draper, and E. S. Vitetta, *Proc. Natl. Acad. Sci. U.S.A.* **105**, 8697 (2008).

<sup>9</sup>E. Pop, D. Mann, J. Cao, Q. Wang, K. Goodson, and H. Dai, *Nano Lett.* **6**, 96 (2006).

<sup>10</sup>C. Yu, L. Shi, Z. Yao, D. Li, and A. Majumdar, *Nano Lett.* **5**, 1842 (2005).

<sup>11</sup>C. L. Kane, E. J. Mele, R. S. Lee, J. E. Fischer, P. Petit, H. Dai, A. Thess, R. E. Smalley, A. R. M. Verschueren, S. J. Tans, and C. Dekker, *Europhys. Lett.* **41**, 683 (1998).

<sup>12</sup>J. E. Fischer, H. Dai, A. Thess, R. Lee, N. M. Hanjani, D. L. Dehaas, and R. E. Smalley, *Phys. Rev. B* **55**, R4921 (1997).

<sup>13</sup>D. Mann, K. E. Pop, J. Cao, Q. Wang, K. Goodson, and H. J. Dai, *J. Phys. Chem. B* **110**, 1502 (2006).

<sup>14</sup>E. Pop, D. Mann, J. Reifenberg, K. E. Goodson, and H. J. Dai, in *IEEE International Electron Devices Meeting (IEDM)*, Washington, D.C. (IEEE, New York, 2005), pp. 253–256.

<sup>15</sup>X. Zhou, J. Y. Park, S. Huang, J. Liu, and P. L. McEuen, *Phys. Rev. Lett.* **95**, 146805 (2005).

<sup>16</sup>Z. Yao, C. L. Kane, and C. Dekker, *Phys. Rev. Lett.* **84**, 2941 (2000).

<sup>17</sup>D. Mann, A. Javey, J. Kong, Q. Wang, and H. Dai, *Nano Lett.* **3**, 1541 (2003).

<sup>18</sup>F. Arai, C. Ng, P. Liu, L. Dong, Y. Imaizumi, and K. Maeda, *Proceedings of the Fourth IEEE Conference on Nanotechnology*, 2004 (unpublished), pp. 146–148.

<sup>19</sup>B. Q. Wei, R. Vajtai, and P. M. Ajayan, *Appl. Phys. Lett.* **79**, 1172 (2001).

<sup>20</sup>M. A. Kuroda, A. Cangelaris, and J. P. Leburton, *Phys. Rev. Lett.* **95**, 266803 (2005).

<sup>21</sup>M. A. Kuroda and J. P. Leburton, *Appl. Phys. Lett.* **89**, 103102 (2006).

<sup>22</sup>J. Y. Park, S. Rosenblatt, Y. Yaish, V. Sazonova, H. Ustunel, S. Braig, T. A. Arias, P. W. Brouwer, and P. L. McEuen, *Nano Lett.* **4**, 517 (2004).

<sup>23</sup>E. Pop, D. Mann, K. Goodson, and H. Dai, *J. Appl. Phys.* **101**, 093710 (2007).

<sup>24</sup>V. A. Sazonova, 2006, “A tunable carbon nanotube resonator,” Ph.D. thesis, Cornell University, Ithaca, NY.

<sup>25</sup>V. Sazonova, Y. Yaish, H. Ustunel, D. Roundy, T. A. Arias, and P. L. McEuen, *Nature (London)* **431**, 284 (2004).

<sup>26</sup>Certain commercial materials and equipment are identified in order to specify adequately experimental procedures. In no case does such identification imply recommendation or endorsement by the National Institute of Standards and Technology, nor does it imply that the items identified are necessarily the best available for the purpose.

<sup>27</sup>J. P. Chandler, 1975, <http://qcpe.chem.indiana.edu/> (enter QCPE code No. 66).

<sup>28</sup>R. Hooke and T. A. Jeeves, *J. Assoc. Comput. Mach.* **8**, 212 (1961).

<sup>29</sup>J. A. Nelder and R. Mead, *Comput. J.* **7**, 308 (1975).

<sup>30</sup>P. S. Na, H. Kim, H. M. So, K. J. Kong, H. Chang, B. H. Ryu, Y. Choi, J. O. Lee, B. K. Kim, J. J. Kim, and J. Kim, *Appl. Phys. Lett.* **87**, 093101 (2005).

<sup>31</sup>T. Yamamoto, S. Watanabe, and K. Watanabe, *Phys. Rev. Lett.* **92**, 075502 (2004).